Photoinduced electron transfer at liquid|liquid interfaces. Part VII. Correlation between self-organisation and structure of water-soluble photoactive species

ARTICLE *in* JOURNAL OF ELECTROANALYTICAL CHEMISTRY · DECEMBER 2003

Impact Factor: 2.87 · DOI: 10.1016/j.jelechem.2003.07.009

4 AUTHORS, INCLUDING:

Henrik Jensen
University of Copenhagen
88 PUBLICATIONS **1,839** CITATIONS
SEE PROFILE

David J. Fermín
University of Bristol
109 PUBLICATIONS **1,820** CITATIONS
SEE PROFILE

Hubert H Girault
École Polytechnique Fédérale de Lausanne
556 PUBLICATIONS **13,787** CITATIONS
SEE PROFILE

Available online at www.sciencedirect.com
SCIENCE DIRECT®
Journal of Electroanalytical Chemistry 560 (2003) 143–149
Journal of Electroanalytical Chemistry
www.elsevier.com/locate/jelechem

Photoinduced electron transfer at liquid|liquid interfaces. Part VII. Correlation between self-organisation and structure of water-soluble photoactive species

Nicolas Eugster, Henrik Jensen, David J. Fermín *, Hubert H. Girault

Laboratoire d'Electrochimie Physique et Analytique, Institut de Chimie Moléculaire et Biologique, Ecole Polytechnique Fédérale de Lausanne, CH-1015 Lausanne, Switzerland

Received 1 May 2003; received in revised form 30 June 2003; accepted 7 July 2003

Abstract

The self-organisation of a variety of dyes at the water|1,2-dichloroethane interface was studied by admittance measurements, photocurrent–potential curves and light polarisation anisotropy of the photocurrent. The heterogeneous photo-oxidation of ferrocene was studied at interfaces sensitised by Sn(IV) *meso*-tetra-(4-carboxyphenyl) porphyrin dichloride (SnTPPC), chlorin e-6, protoporphyrin IX (protoIX) and Fe(III) protoporphyrin IX chloride (Fe-protoIX). Cyclic voltammograms and capacitance voltage curves exhibit different features associated with the self-assembly of the dye species at the liquid|liquid boundary. In the case of SnTPPC, the capacitance curves displayed the characteristic responses commonly associated with the specific adsorption of ionic species. On the other hand, chlorin e-6, protoIX and Fe-protoIX show rather complex behaviour suggesting not only changes in the excess charge but also in the dielectric permittivity of the interface. Differences in the photocurrent efficiency were also observed under the same experimental conditions. The relative magnitude of the photocurrent responses were rationalised in terms of the phenomenological electron transfer rate constant, the photon capture cross-sections and the lifetime of the triplet state as obtained from nanosecond flash photolysis. Finally, the average molecular orientation of the adsorbed photoactive species was estimated from the photocurrent dependence on the angle of light polarisation in total internal reflection. The results show a clear correlation between the orientation of the transition dipole and the distribution of the peripheral carboxyl groups responsible for the hydrophilic nature of the dyes.

Keywords: Photocurrent; ITIES; Porphyrin; Self-assembly; Molecular orientation

1. Introduction

The photoreactivity of dyes towards heterogeneous electron transfer across polarisable molecular interfaces can be conveniently studied by photoelectrochemical methods [1–3]. In the case of interfaces between two immiscible electrolyte solutions (ITIES), the photoinduced electron transfer between water-soluble dyes and redox couples in the organic phase manifests itself by photocurrent responses under potentiostatic conditions [1,4–9]. The photoresponses arise from the charge separation across the liquid|liquid boundary on the microsecond timescale followed by the diffusion of products and the regeneration of the dye species specifically adsorbed at the liquid|liquid boundary [8,9]. The interfacial charge separation is determined by the competition between the photoinduced electron transfer and the relaxation of the excited state. This competition introduces a dependence of the photocurrent on the applied Galvani potential difference across the ITIES [5,7–9].

The specific adsorption of the dye species at the molecular boundary is a key aspect in their heterogeneous photoreactivity. We have studied the adsorption of water-soluble dyes including zinc(II) *meso*-tetra

* Corresponding author. Tel.: +41-21-693-3162; fax: +41-21-693-3667.
E-mail address: david.fermin@epfl.ch (D.J. Fermín).
URL: http://dcwww.epfl.ch/le/.

0022-0728/$ - see front matter © 2003 Elsevier B.V. All rights reserved.
doi:10.1016/j.jelechem.2003.07.009

(4-carboxyphenyl) porphyrin (ZnTPPC), zinc(II) tetra(*N*-methyl-4pyridinium) porphyrin (ZnTMPyP) and Zn(II) *meso*-tetra(4-sulphonatophenyl) porphyrin (ZnTPPS) employing a variety of techniques such as impedance spectroscopy [4], potential modulated fluorescence [10,11], second harmonic generation [12,13] and quasi-elastic laser scattering [13]. These studies have shown that the porphyrin coverage can be affected by the applied potential. At high coverage, the formation of aggregates can take place at the interfacial boundary. A particularly interesting case is the ZnTPPC adsorption at the water|DCE interface, in which the extent of the porphyrin aggregation can be reversibly controlled by tuning the Galvani potential difference [4,5,13]. In the present communication, we shall examine the specific adsorption of different porphyrin dyes by studying the effect of the polarisation of the incident light on the photocurrent responses. Photocurrent anisotropy on the light polarisation in total internal reflection allows the estimation of the average angle between the plane containing the transition dipoles and the surface normal [14]. The results obtained for Sn(IV) *meso*-tetra(4-carboxyphenyl) porphyrin dichloride (SnTPPC), chlorin e-6, protoporphyrin IX (protoIX) and Fe(III) protoporphyrin IX chloride (Fe-protoIX) reveal distinctive adsorption modes for these dyes at the water|DCE interface. The average orientation will be rationalised in terms of the molecular structure of the sensitisers illustrated in Fig. 1.

2. Experimental

All reagents employed were analytical grade. The dyes SnTPPC (Porphyrin Products), chlorin e-6 (Frontier Scientific), Fe-protoIX (Porphyrin Products) and protoIX (Aldrich) were employed without further purification. Bis(triphenyl-phosphoranylidene) ammonium tetrakis(pentafluorophenyl) borate (BTPPATPFB) and Li_2SO_4 were employed as the organic and aqueous phase supporting electrolytes, respectively. The pH of the aqueous electrolyte was adjusted to 7. The preparation of BTPPATPFB has been reported elsewhere [5]. The composition of the electrolyte solutions is presented in Fig. 2. The water|1,2-dichloroethane (DCE) interface was polarised via a custom-built four-electrode potentiostat. The Galvani potential difference was estimated by assuming that the minimum of the differential capacitance curve corresponds to $\Delta_o^w\phi = 0$.

Photocurrent–potential curves were measured in a three-compartment glass cell provided with two platinum counter-electrodes and two luggin capillaries for

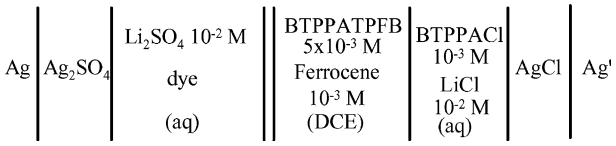

Fig. 2. Schematic representation of the electrochemical cell.

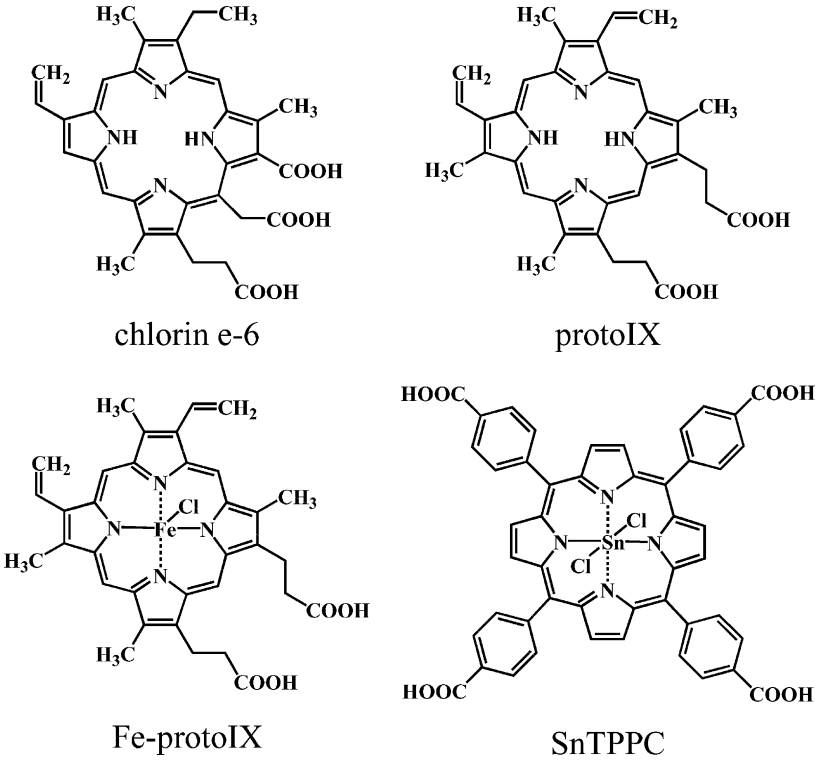

Fig. 1. Molecular structure of the sensitisers chlorin e-6, protoporphyrin IX (protoIX), Fe(III)-protoporphyrin IX chloride (Fe-protoIX) and Sn(IV) *meso*-tetra(4-carboxyphenyl) porphyrin dichloride (SnTPPC).

the reference electrodes. The geometrical surface area was 1.53 cm^2 and the uncompensated resistance between the two reference electrodes was typically of 100 Ω. The liquid|liquid junction was illuminated with the 442 nm line of a He–Cd laser (Omnichrome Series 74). The laser beam was defocused in order to illuminate the whole interface with an average photon flux of 8.7×10^{16} $cm^{-2}\,s^{-1}$.

Photocurrent measurements as a function of the polarisation of the incoming light were measured under total internal reflection from the organic phase, fixing an incident angle of 75° with respect to the surface normal. The cell employed for these studies features a piston burette, which allows a careful positioning of the liquid|liquid junction (surface area of 0.22 cm^2) [10]. The polarisation of the incoming laser beam was controlled by placing a polariser at the output of the laser head followed by a remote-controlled rotator (Aerotech Unidex 100) equipped with a half-wave plate.

Triplet state lifetimes were estimated by flash photolysis using a Nd:YAG laser as the excitation source, providing 6 ns pulses at a repetition rate of 30 Hz. An OPO was used to tune the pump wavelength to 600 nm. The probe light intensity from a Xe lamp was measured by a fast photomultiplier after passing through a monochromator. Data were averaged over 1000 laser shots by a 1 GHz band-pass digital oscilloscope.

3. Results and discussion

3.1. Specific adsorption and photoreactivity of the sensitisers at the water|DCE interface

The voltammetric responses of the ionic dyes at the water|DCE interface are contrasted in Fig. 3. In the presence of chlorin e-6 and protoIX, the voltammetric responses associated with the transfer from water to DCE can be observed at negative Galvani potential differences ($\Delta^{w}_{o}\phi$). The half-wave transfer potential for chlorin e-6 and protoIX were estimated around −0.35 and −0.20 V, respectively. On the other hand, no clear transfer responses are observed for Fe-protoIX and SnTPPC within the polarisable window. The differences in the transfer behaviour of the dyes reveal various degrees of hydrophobicity, which can be expressed in terms of the standard Gibbs energy of ion transfer ($\Delta G^{o,w\to o}_{tr,i}$),

$$\Delta G^{o,w\to o}_{tr,i} = z_i F \Delta^{w}_{o}\phi^{o}_{i} \quad (1)$$

where z_i and $\Delta^{w}_{o}\phi^{o}_{i}$ correspond to the charge and standard transfer potential of the ion "i". Taking the half wave potential of the voltammetric peaks as the standard ion transfer potentials in Fig. 3, it follows that $\Delta G^{o,w\to o}_{tr,PPIX} < \Delta G^{o,w\to o}_{tr,CE-6} < \Delta G^{o,w\to o}_{tr,FePPIX}, \Delta G^{o,w\to o}_{tr,SnTPPC}$. In the case of chlorin e-6, a pre-peak signal is observed at −0.21 V indicating that the dye is specifically adsorbed at the liquid|liquid boundary prior to the transfer from water to DCE [7,10,13]. The peak-to-peak separation of the transfer signal is approximately 40 mV, which is larger than the 19.7 mV corresponding to the fully deprotonated form of chlorin e-6. Indeed, it is expected that most of the chlorin e-6 species are deprotonated at pH 7 [15]. The large peak-to-peak separation may arise from the uncompensated resistance between the two reference electrodes and the convolution of the transfer and adsorption responses. On the other hand, the peak-to-peak separation associated with the transfer of proto-IX does approach the 29.5 mV consistent with the dianionic form of the dye. The width of the voltammetric signal also suggests that proto-IX is specifically adsorbed at the interface at potential close to the transfer region.

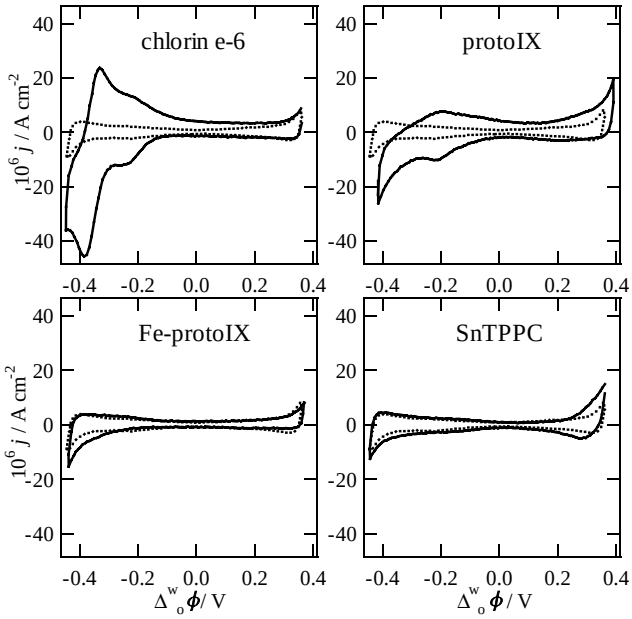

Fig. 3. Cyclic voltammograms in the absence (dotted lines) and in the presence of chlorin e-6, protoIX, Fe-protoIX and SnTPPC at 50 mV s^{-1}. The concentration of the dye was 10^{-4} mol dm^{-3}. The composition of the electrochemical cell is as indicated in Fig. 2.

The specific adsorption of ionic species at the liquid|liquid boundary manifests itself by perturbations of the differential capacitance as exemplified in Fig. 4. The differential capacitance was estimated from admittance measurements at 12 Hz and an amplitude of 4 mV rms. The symmetrical potential dependence of the capacitance around the potential of zero charge for the water|DCE junction is strongly affected in the presence of all four dyes. In the case of SnTPPC the minimum of the capacitance shifts to positive potentials, showing a steep increment of the capacitance towards negative potentials. This behaviour is consistent with the specific adsorption of hydrophilic anionic species featuring a strong affinity for the liquid|liquid boundary [4,5,16,17].

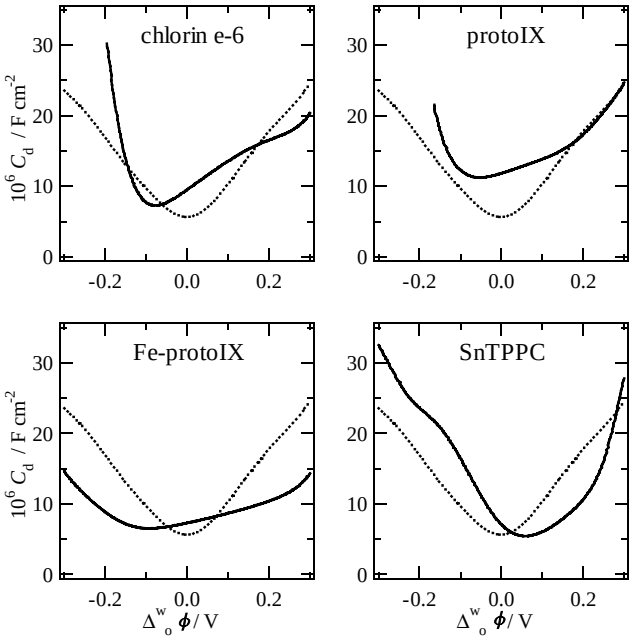

Fig. 4. Differential capacitance–potential curves of the water|DCE interface in the presence of 10^{-4} mol dm^{-3} of chlorin e-6, protoIX, Fe-protoIX and SnTPPC. The dotted line corresponds to the capacitance in the absence of the dye species.

On the other hand, substantial changes to the capacitance–potential curves are observed upon addition of protoIX, Fe-protoIX or chlorin e-6 to the aqueous phase. The minimum of the capacitance is observed at negative potentials. The potential dependence appears somewhat weak at more positive values, suggesting a change in the interfacial relative permittivity. These phenomena have been observed during the formation of a dense surfactant-type monolayer at the liquid|liquid boundary [18].

From the capacitance curves in Fig. 4, it is clear that the four dyes investigated exhibit strong specific adsorption, introducing substantial changes in the potential distribution across the interface. In order to extract quantitative information from the capacitance–potential curves, processes such as interfacial protonation, ion-pairing and dye aggregation should be taken into account. Indeed, acid–base equilibria involving some of these dyes are rather complex due to the aggregation processes and the low solubility of the protontated forms [15,19,20]. In the case of SnTPPC, it is expected that the pK_a of the peripheral carboxyl groups is close to that observed for the free base, i.e., 5.8 [20]. Our previous studies revealed that the self-assembly of the ZnTPPC at the water|DCE junction is extremely sensitive to the pH in the aqueous phase [14]. Photocurrent and impedance data showed that the adsorption of ZnTPPC takes place only at pH lower than 9, indicating that the species adsorbed at the interface are not fully deprotonated. These results suggest that a key phenomenon involved in the stabilisation of the carboxyphenyl derivatised porphyrin is the formation of cooperative hydrogen bonds. As discussed in the next section, the cooperative hydrogen bonding determines the orientation of SnTPPC at the liquid|liquid boundary to a large extent.

Photocurrent–potential curves for the various anionic dyes in the presence of ferrocene in the organic phase are contrasted in Fig. 5. The measurements were performed using lock-in detection under chopped illumination at 12 Hz. The photocurrent responses were effectively in-phase with the light perturbation in the potential range examined. At more positive potentials, phase shifts were observed due to the *RC* relaxation of the cell [5,21]. The photocurrent increases with increasing $\Delta^w_o \phi$ with an onset potential close to −0.1 V for chlorin e-6, protoIX and Fe-protoIX. The onset potential appears slightly more negative in the case of SnTPPC, reflecting the different adsorption properties observed in capacitance–potential curves. In order to rationalise the difference in the photoresponses, it should be considered that the photocurrent magnitude is determined by the surface concentration of the dye at the liquid|liquid boundary, the photon capture cross-section (σ) and the quantum yield of the heterogeneous photochemical reaction [4]. The quantum yield is a function of the phenomenological pseudo-first order electron transfer rate constant (k_{et}) and the characteristic rate constant of excited state relaxation (k_d). Our previous studies suggested that the transient time for the heterogeneous electron transfer is on the microsecond timescale. This rate is largely influenced by the redox potential of the excited state, the Galvani potential difference between the two phases and the distance separating the reactants [5,7–9]. This characteristic time constant for the electron transfer indicates that the photoreaction involves a reductive quenching of the triplet state. Consequently, the overall photocurrent quantum efficiency is also determined by the efficiency of intersystem crossing of the adsorbed dye species.

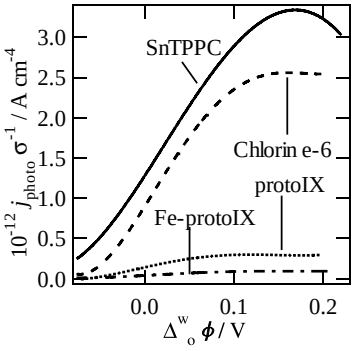

Fig. 5. Photocurrent–potential curves normalised for the photon capture cross-section for each of the dyes.

Table 1
Photon capture cross-section at 442 nm and rate constant for the decay of the triplet state for the various dyes studied

	Chlorin e-6	Proto IX	Fe-proto IX	SnTPPC
10^{17} σ/cm^{-2}	0.49	5.35	2.07	1.50
10^{-5} k_d/s^{-1}	4.13	0.12	–	1.96

The values for σ at 442 nm and k_d associated with the triplet state are summarised in Table 1. Flash photolysis was employed for estimating k_d in aqueous solution with the composition indicated in Fig. 2. To account for the difference in light absorption, the photocurrent in Fig. 5 was normalised by σ. In the case of Fe-protoIX, the photocurrent responses are substantially smaller than for the other dyes under identical conditions. This difference in the photocurrent efficiency arises from the fact that the lifetime of Fe-protoIX is less than 50 ps due to a deactivation mechanism involving short-lived porphyrin-metal charge-transfer and ligand field states of lower energy [22]. The timescale of this reaction is orders of magnitude shorter than the characteristic transient time for electron transfer across the liquid|liquid boundary [8]. Consequently, the excited state relaxes before the electron transfer from ferrocene in DCE takes place. We believe that a part of the photoresponses observed for Fe-protoIX is linked to the presence of demetalated species in the aqueous phase. On the other hand, as the efficiency of intersystem crossing for the other dyes is above 75%, the difference in the photocurrent magnitude is expected to be determined by the two remaining factors: (i) surface concentration of the dye species and (ii) competition between triplet state relaxation and the heterogeneous electron transfer. SnTPPC exhibits a larger photocurrent than Chlorin e-6, which is consistent with the slower decay rate constant obtained for the former. However, it should be considered that the photophysical properties of these dyes at the liquid|liquid boundary may differ from those measured in bulk solution. Local pH as well as aggregation phenomena can introduce changes in the absorption of the dye and lifetime of the excited state. Unexpectedly, protoIX shows a rather small photocurrent despite the relatively slow excited state decay. From the voltammetric and capacitance data illustrated in Figs. 3 and 4, in addition to the molecular orientation studies described in the next section, it could be envisaged that the adsorption properties of protoIX and chlorin e-6 are comparable. Consequently, the low photocurrent magnitudes for protoIX can be associated with a slow heterogeneous electron transfer reaction.

3.2. Average orientation of the adsorbed photoactive dyes

The photocurrent dependence on the angle of polarisation of the incoming light in total internal reflection is exemplified in Fig. 6 for the case of SnTPPC at various

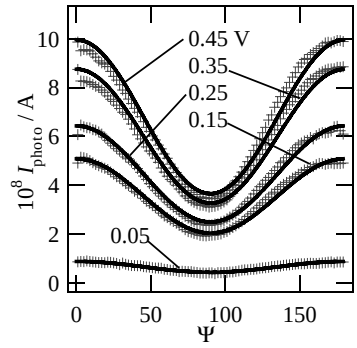

Fig. 6. Photocurrent responses as a function of the angle of polarisation of the incoming light in the presence of 10^{-6} mol dm^{-3} of SnTPPC at various Galvani potential differences. The solid lines are obtained from Eq. (2), taking C and ξ as adjustable parameters.

Galvani potential differences. The photocurrent anisotropy with the light polarisation indicates that the transition dipoles of the photoactive species exhibit a well-defined orientation with respect to the interfacial plane. In the case of SnTPPC, the transition dipoles are orthogonal and located in the plane of the porphyrin ring. The minimum in the photocurrent for p-polarised light suggests that the porphyrin species adopt a rather flat orientation with respect to the interfacial plane. As the Galvani potential difference is shifted to more negative potentials, the photocurrents exhibit a weaker dependence on the polarisation angle, suggesting a change in the orientation from a coplanar to a more upright position.

The photocurrent dependence on the polarisation angle (Ψ) allows the estimation of the average tilting angle between the dipole transition and the surface normal (ξ). Considering that the reflection plane from the interface coincides with the adsorption plane of the porphyrins, the photocurrent density dependence on Ψ is given by [14,23,24],

$$j_{photo}(\xi)/C = \sin^2(\xi)\cos^2(\Psi) + [\cos^2(\beta)\sin^2(\xi) + 2\sin^2(\beta)\cos^2(\xi)]\sin^2(\Psi) \quad (2)$$

where β corresponds to the incident angle of illumination, i.e., 75°, and C is a proportionality factor depending on the photon flux to the interface and the photocurrent conversion efficiency. Expression (2) is strictly valid in the case that the adsorption plane of the photoactive porphyrins coincides with the reflection plane. Indeed, the magnitude of the photocurrent shows

very little dependence on variations of the angle β in total internal reflection, providing clear evidence that the flux of photoinduced electron transfer is independent of the penetration depth of light. It should also be considered that this expression allows the estimation of the average angle between the surface normal and the plane containing the two orthogonal dipole transitions. While the non-symmetric porphyrins in Fig. 1 exhibit transition dipoles of different magnitudes in the plane of the ring, the SnTPPC does feature orthogonal dipoles of the same magnitude. It should be stressed that Eq. (2) provides only an average value of the angle between the plane containing the transition dipoles and the surface normal. This analysis is unable to determine the orientation of the effective dipole moment of the molecule, e.g., it cannot be established directly whether the peripheral carboxyl groups are pointing towards the aqueous or organic phase. The continuous line in Fig. 6 corresponds to the fits to eq. (8), taking C and ξ as adjustable parameters.

The dependence of the average tilting angle on the concentration of SnTPPC in the aqueous phase at various potentials is displayed in Fig. 7a. The orientation of the adsorbed SnTPPC shows a clear dependence on the bulk concentration at potentials close to 0 V. At positive potentials, the concentration dependence becomes weaker and the porphyrins adopt a rather coplanar orientation with respect to the interfacial plane. Rough estimations of the excess concentration from the differential capacitance suggest that this change in orientation takes place in the potential region where the coverage is smaller than 10% of a monolayer. On the other hand, a significant decrease in the angle ξ with decreasing potential indicates a change of the porphyrin orientation towards a more upright position. These changes in the average orientation occur concomitantly with the increase in the surface coverage of the porphyrin. This correlation suggests that the adsorbed SnTPPC is organised in a fashion minimising the electrostatic repulsion from the peripheral carboxyl group and enhancing the interaction between the porphyrin rings. Indeed, these results are fully compatible with recent second harmonic generation studies of the ZnTPPC adsorption at the water|DCE interface, showing the formation of aggregates at negative potentials [13,14].

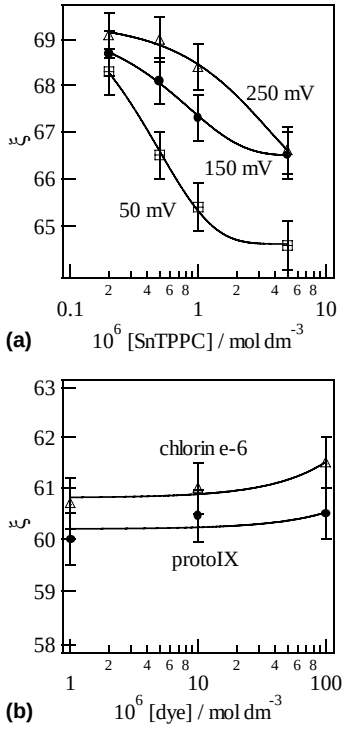

Fig. 7. Average tilting angle between the transition dipole and the surface normal as a function of the dye concentration for SnTPPC (a) as well as chlorin e-6 and protoIX (b). The angle ξ was found to be dependent on the applied potential only in the case of SnTPPC. Chlorin e-6 and protoIX show very similar tilting angles, which are very little dependent on the dye concentration.

The average orientations of chlorin e-6 and protoIX do exhibit different behaviour with respect to SnTPPC as illustrated in Fig. 7b. For these two dyes, the photocurrent dependence on the polarisation angle is unaffected by the Galvani potential difference. It is also observed that the average orientation is weakly dependent on the concentration, indicating that lateral interactions between the adsorbed species are negligible under these conditions. As previously suggested for Cu-chlorophyllin, the asymmetric distribution of the carboxyl groups around the chromophore ring introduces amphiphillic properties to the dye [24]. This is consistent with the more upright orientation of chlorin e-6 and protoIX with respect to SnTPPC.

Finally, the average molecular orientation estimated for protoIX appeared somewhat different from previous analysis based on second harmonic generation [25]. The source of the discrepancy remains to be clarified. Taking into consideration the low values of the second order hyperpolarisability exhibited by these porphyrins [26], negligible SHG responses would be obtained for the average orientation extracted from our photocurrent analysis. In the light of the intense static electric fields at the polarised liquid|liquid boundary, it could be argued that the origin of the SHG signal is related to the quadrupolar rather than the χ^2 component [13]. We are currently investigating this issue of crucial importance for understanding interfacial reactivity at these molecular junctions.

4. Conclusions

The reactivity of dyes towards heterogeneous photoinduced electron transfer across liquid|liquid inter-

faces is closely linked to their structure and photophysical properties. Comparisons between the interfacial behaviour of SnTPPC, chlorin e-6, protoIX and Fe-protoIX reveal an interesting correlation between the specific adsorption and the distribution of the peripheral carboxyl groups around the chromophore ring. The dyes exhibit a strong affinity for the liquid|liquid boundary that manifests itself by changes in the differential capacitance even at potentials substantially more positive than the formal ion transfer potential. The differential capacitance shows very complex behaviour especially in the case of protoIX, Fe-protoIX and chlorin e-6. These three dyes exhibit a very similar structure, featuring carboxyl groups located at one side of the porphyrin ring. The high values of the capacitance with respect to that of the dye-free interface, even at potentials close to the pzc, suggest adsorption behaviour similar to that observed for amphiphilic molecules. On the other hand, the coverage of SnTPPC appears to show a strong potential dependence over the whole polarisable window.

For all the dyes studied, the photocurrent responses increase with increasing Galvani potential difference. This behaviour confirms that the phenomenological rate constant for the heterogeneous electron transfer increases as the applied potential is tuned towards positive values. The photocurrent in the presence of protoIX, Fe-protoIX and chlorin e-6 shows a common onset potential; however the magnitude is substantially smaller for the Fe-protoIX sensitised interface. This difference is associated with the short lifetime of the excited state due to the internal singlet quenching by the orbitals associated with the Fe centre. The more negative onset potential for SnTPPC further confirms the different adsorption properties with respect to the other dyes.

Finally, photocurrent polarisation anisotropy revealed that the specifically adsorbed porphyrins feature a well-defined average orientation at the liquid|liquid boundary. In the case of SnTPPC, changes in the applied potential can induce variations of the average tilting angle of more than 2° at low porphyrin concentrations. By contrast, the orientation of protoIX and chlorin e-6 is effectively independent of the applied potential and bulk concentration. These results suggest that the organisation of the protoIX and chlorin e-6 is mostly determined by specific interactions between the liquid|liquid boundary and the inhomogeneous solvation properties of the dyes. As we mentioned previously, these properties are determined by the asymmetric distribution of the carboxyl groups. On the other hand, lateral interactions between the adsorbates are determinant factors in the organisation of SnTPPC. These interactions include lateral repulsion, cooperative hydrogen bonding and aggregation [13,14].

Acknowledgements

This work has been sponsored by the Fonds National Suisse de la Recherche Scientifique (Project 2000-067050.01). We acknowledge technical support by Valérie Devaud. The Laboratoire d'Electrochimie Physique et Analytique is part of the European TMR network SUSANA (Supramolecular Self-Assembly of Interfacial Nanostructures).

References

[1] D.J. Fermín, Z.F. Ding, H.D. Duong, P.F. Brevet, H.H. Girault, Chem. Commun. (1998) 1125.
[2] D.J. Fermín, R. Lahtinen, in: A. Volkov (Ed.), Liquid Interfaces in Chemical, Biological, and Pharmaceutical Applications, vol. 95, Marcel-Dekker, Boca Raton, 2001, p. 179.
[3] D.J. Fermín, H. Jensen, H.H. Girault, in: E.J. Calvo (Ed.), Encyclopedia of Electrochemistry, Interfacial Kinetics and Mass Transport, vol. 2, Wiley-VCH, New York, 2003, p. 360.
[4] D.J. Fermín, Z.F. Ding, H.D. Duong, P.F. Brevet, H.H. Girault, J. Phys. Chem. B 102 (1998) 10334.
[5] D.J. Fermín, H.D. Duong, Z.F. Ding, P.F. Brevet, H.H. Girault, Phys. Chem. Chem. Phys. 1 (1999) 1461.
[6] D.J. Fermín, H.D. Duong, Z.F. Ding, P.F. Brevet, H.H. Girault, Electrochem. Commun. 1 (1999) 29.
[7] D.J. Fermín, H.D. Duong, Z.F. Ding, P.F. Brevet, H.H. Girault, J. Am. Chem. Soc. 121 (1999) 10203.
[8] N. Eugster, D.J. Fermín, H.H. Girault, J. Phys. Chem. B 106 (2002) 3428.
[9] N. Eugster, D.J. Fermín, H.H. Girault, J. Am. Chem. Soc. 125 (2003) 4862.
[10] H. Nagatani, R.A. Iglesias, D.J. Fermín, P.F. Brevet, H.H. Girault, J. Phys. Chem. B 104 (2000) 6869.
[11] H. Nagatani, D.J. Fermín, H.H. Girault, J. Phys. Chem. B 105 (2001) 9463.
[12] H. Nagatani, A. Piron, P.F. Brevet, D.J. Fermín, H.H. Girault, Langmuir 18 (2002) 6647.
[13] H. Nagatani, Z. Samec, P.F. Brevet, D.J. Fermín, H.H. Girault, J. Phys. Chem. B 107 (2003) 786.
[14] H. Jensen, J.J. Kakkassery, H. Nagatani, D.J. Fermín, H.H. Girault, J. Am. Chem. Soc. 122 (2000) 10943.
[15] B. Cunderlikova, L. Gangeskar, J. Moan, J. Photochem. Photobiol. B-Biol. 53 (1999) 81.
[16] S. Frank, W. Schmickler, J. Electroanal. Chem. 500 (2001) 491.
[17] L.I. Daikhin, A.A. Kornyshev, M. Urbakh, J. Electroanal. Chem. 500 (2001) 461.
[18] Z. Samec, Chem. Rev. 88 (1988) 617.
[19] B. Cunderlikova, M. Kongshaug, L. Gangeskar, J. Moan, Int. J. Biochem. Cell Biol. 32 (2000) 759.
[20] N.C. Maiti, S. Mazumdar, N. Periasamy, J. Phys. Chem. B 102 (1998) 1528.
[21] R. Lahtinen, D.J. Fermín, K. Kontturi, H.H. Girault, J. Electroanal. Chem. 483 (2000) 81.
[22] K. Kalyanasundaram, Photochemistry of Polypyridine and Porphyrin Complexes, Academic Press, London, 1992.
[23] N. Ohta, S. Matsunami, S. Okazaki, I. Yamazaki, Langmuir 10 (1994) 3909.
[24] H. Jensen, D.J. Fermín, H.H. Girault, Phys. Chem. Chem. Phys. 3 (2001) 2503.
[25] J. Perrenoud-Rinuy, P.F. Brevet, H.H. Girault, Phys. Chem. Chem. Phys. 4 (2002) 4774.
[26] A. Sen, P.C. Ray, P.K. Das, V. Krishnan, J. Phys. Chem. 100 (1996) 19611.